HHS Public Access

Author manuscript

Cancer Immunol Res. Author manuscript; available in PMC 2016 June 01.

Published in final edited form as:

Cancer Immunol Res. 2015 June ; 3(6): 620–630. doi:10.1158/2326-6066.CIR-14-0201.

PD-1+Tim-3+ CD8+ T Lymphocytes Display Varied Degrees of Functional Exhaustion in Patients with Regionally Metastatic Differentiated Thyroid Cancer

Jill J. Severson[*], **Hilary S. Serracino**[†], **Valerica Mateescu**[†], **Christopher D. Raeburn**[§,‡], **Robert C.McIntyre Jr.**[§,‡], **Sharon B. Sams**[†,‡], **Bryan R. Haugen**[*,†,‡], and **Jena D. French**[*,‡]

[*]Department of Medicine, Division of Endocrinology, Metabolism, and Diabetes, University of Colorado, Anschutz Medical Campus, Aurora, CO 80045

[†]Department of Pathology, University of Colorado, Anschutz Medical Campus, Aurora, CO 80045

[§]Department of Surgery, University of Colorado, Anschutz Medical Campus, Aurora, CO 80045

[‡]University of Colorado Cancer Center, University of Colorado, Anschutz Medical Campus, Aurora, CO 80045

Abstract

Regional metastatic differentiated thyroid cancer (mDTC) provides a unique model in which to study the tumor-immune interface. These lymph node (LN) metastases persist for years, generally without progression to distant metastases. While the immune system likely impedes disease progression, it is unsuccessful in eliminating disease. Our previous studies revealed that programmed death-1 (PD-1)$^+$ T cells were enriched in tumor-involved lymph nodes (TILN). Tumor-associated leukocytes and tumor cells were collected from grossly involved LNs from 12 patients to further characterize the phenotype and functional potential of mDTC-associated PD-1$^+$ T cells. PD-1$^+$CD4$^+$ and PD-1$^+$CD8$^+$ T cells were enriched in 8/12 TILN samples. PD-1$^+$ T cells co-expressed Tim-3 and CD69 and failed to down-regulate CD27. CD8$^+$ T cells, but not CD4$^+$ T cells, from these samples were variably deficient in their ability to produce effector cytokines when compared to control TILNs that lacked resident PD-1$^+$ T cells. PD-1$^+$CD8$^+$ T cells were capable of exocytosis but lacked intracellular perforin. Surprisingly, T-cell proliferative capacity was largely maintained in all samples. Thus, while PD-1 expression by mDTC-associated CD8$^+$ T cells was associated with dysfunction, exhaustion was not complete. Notably, molecular markers of exhaustion did not translate to dysfunction in all samples or in CD4$^+$ T cells. Regulatory T (Treg) cells, PD-L1, and galectin-9 were commonly found in mDTC and likely contributed to the initiation of T-cell exhaustion and disease progression. Therapies that release the effects of PD-1 and Tim-3 and reduce the suppressive effects of Tregs may encourage tumor elimination in patients with mDTC.

Corresponding Author: Jena D. French University of Colorado, Anschutz Medical Campus 12801 E. 17th Ave RC1 South, 7401D, Mail Stop 8106 Aurora, CO 80045 Phone: 303-724-3928 Fax: 303-724-3920 jena.french@ucdenver.edu.

Conflict of Interest: None

Keywords

Thyroid Cancer; Metastasis; PD-1; Exhaustion; Regulatory T cells

Introduction

More than 500,000 people in the United States have a diagnosis of thyroid cancer, and the incidence is steadily growing, with an estimated 62,000 new cases in 2014 (1). Although localized differentiated thyroid cancer (DTC) is generally managed by surgery and radioactive iodine therapy, approximately 10% of patients develop progressive invasive primary disease and 5% develop distant metastases (1). 20%–30% of patients with DTC develop persistent or recurrent disease, most commonly in locoregional lymph nodes (LN), requiring additional surgical intervention with increased morbidity and expense (2). Patients with aggressive DTC that are resistant to standard treatments may be excellent candidates for innovative adjuvant therapies, including immune-modulating approaches.

DTC provides a unique model in which to study the interplay between the immune response and the metastatic tumor. LN metastases are common in patients with DTC (>60%) (3). These regional metastases are thought to persist for years, generally without progression to distant metastasis. The 5-year survival rate for these patients is 97.4%, only slightly reduced compared to the 99.9% survival rate observed in patients with localized disease. In contrast, regional LN involvement in patients with lung, melanoma, or breast cancer indicates a significantly reduced rate of survival compared to localized disease (53.5% to 26.1%, 98.3% to 62.4%, and 98.6% to 84.4%, respectively) (1). Despite their presumed indolent nature, DTC metastases are not eliminated by the immune system, suggesting that the immune response may be compromised. In support of this theory, our previous studies revealed that regulatory T cells (Treg) and Programmed Death-1 $(PD\text{-}1)^+$ T cells are elevated in tumor-involved lymph nodes (TILN) and may contribute to disease severity and recurrence (4).

T-cell exhaustion, which was originally described in models of chronic viral infections, is now established as an important mechanism of immune evasion in cancer. Exhausted T cells are characterized by the sustained expression of one or more inhibitory molecule [e.g., PD-1, cytotoxic T-lymphocyte antigen-4 (CTLA-4), and T-cell immunoglobulin and mucin domain 3 (Tim-3)]. These cells become increasingly dysfunctional during chronic antigen exposure, with loss of IL2 production and reduced *ex vivo* proliferative and cytotoxic potential preceding the loss of TNFα and IFNγ production. Exhaustion culminates in deletion by apoptosis (5, 6). Exhausted $CD8^+$ T cells display a unique expression pattern of activation markers and cytokine receptors (7). For example, these cells fail to down-regulate CD27, which is normally reduced upon T-cell activation. Furthermore, exhausted T cells maintain reduced levels of CD127, which is required for the survival of normal memory T cells. Varied degrees of $CD8^+$ T-cell exhaustion have been reported in melanoma, ovarian cancer, lymphoma, chronic lymphocytic leukemia (CLL), and non-small cell lung cancer (NSCLC) (8-17). Co-expression of inhibitory receptors has been associated with a higher degree of dysfunction in both viral and tumor models (10, 18). PD-1 and Tim-3 co-

expression marked the most dysfunctional tumor-specific T-cell subset in peripheral blood (PB) of patients with melanoma (10).

Although $CD4^+$ T-cell exhaustion has not been thoroughly characterized in human cancers, studies in mouse models of chronic viral infection and patients infected with HIV suggest that virus-specific $CD4^+$ cells express multiple inhibitory receptors and are compromised in their ability to produce effector cytokines (19-22). Similar to $CD8^+$ T cells, $CD4^+$ T-cell exhaustion is characterized by sustained CD27 expression and down-regulation of CD127 (20). A recent study using a mouse model of recurrent melanoma revealed that tumor-specific $CD4^+$ T cells expressed multiple inhibitory receptors, including PD-1 and Tim-3 (23). In patients with B-cell lymphoma, tumor-associated $CD4^+$ T cells expressed PD-1 and Tim-3 and displayed reduced capacity for proliferation and cytokine production (17).

In our previous studies, we sampled both uninvolved LNs (UILN) and TILNs from patients with DTC by fine-needle aspirate biopsy to characterize the T-cell milieu (4). Tregs were enriched in TILNs compared to UILNs and increased levels were associated with recurrent disease. Furthermore, PD-1^+ cells were enriched in both $CD4^+$ and $CD8^+$ T-cell subsets in TILNs compared to UILNs and were associated with extranodal invasion. PD-1^+ $CD4^+$ and $CD8^+$ T cells were antigen-experienced memory cells that maintained the ability to produce IFNγ following stimulation with phorbol-12-myristate-13-acetate (PMA) and ionomycin, but failed to fully down-regulate CD27. To further investigate the role of PD-1 and T-cell exhaustion in metastatic DTC (mDTC), we characterized the phenotype and functional capacity of tumor-associated lymphocytes recovered from TILN tissue sections. These studies are the first to investigate $CD4^+$ and $CD8^+$ T-cell functional exhaustion in thyroid cancer.

Materials and Methods

Patients and Histopathologic Parameters

Patients with thyroid cancer undergoing surgical neck dissection for primary or recurrent disease at University of Colorado Hospital between 2012 and 2014 were offered enrollment in this IRB-approved study. 12 patients were enrolled for the study and were confirmed by histopathology or previous medical reports to have conventional papillary thyroid cancer (PTC; patient #2-9), follicular variants (patient #10), or diffuse sclerosing variants (patients #1, 11, and 12). Chronic lymphocytic thyroiditis was evident in patients 1, 2, and 12. Each case was retrospectively assessed for LN involvement, size of metastases, and extranodal extension. Three normal LNs from trauma patients were acquired from the National Disease Research Interchange (Philadelphia, PA). An archived normal LN from a patient with no history of cancer or autoimmune disease was used as a control for immunohistochemistry.

Sample Acquisition and Processing

LNs ranged from 1.5-2.9 cm in greatest diameter and housed visible tumor parenchyma. Each TILN was bisected, and an interior tissue section was donated. Multiple nodes were sampled when available to increase yield. Samples were collected in Hanks Balanced Salt Solution (HBSS) and digested with 2.5 mg/ml Liberase DL and 10,000 U/ml DNase I

(Roche, San Francisco, CA) at 37°C for one hour. Red blood cells were lysed (37°C for 5 minutes; 150mM ammonium chloride, 10mM potassium bicarbonate, and 0.1mM ethylenediaminetetraacetic acid disodium salt dehydrate (EDTA)), and the remaining cells were incubated overnight in media (RPMI 1640 (Gibco), 10% heat-inactivated HI-FBS, 1:500 Penicillin/ Streptomycin (Gibco)). Non-adherent cells (enriched for lymphocytes) were harvested and adherent cells (enriched for tumor cells) were trypsinized (0.25% Trypsin-EDTA; Gibco). Cells were cryopreserved in freezing media (10% Dimethyl sulfoxide (DMSO) in HIFBS at 1-10×10^6 cells/mL). Sample size and tumor/lymphoid composition varied; thus, a complete phenotypic and functional analysis was not attainable for all samples. Normal or patient-matched PB was donated for isolation of mononuclear cells (PBMC) using Lymphoprep™ gradient media (Axis-Shield PoC AS, Oslo, Norway). Normal LNs were manually disaggregated to obtain a single-cell suspension. PB and normal LNs were cryopreserved as described above. Cryopreserved cells were thawed within 6 months of freezing.

Antibodies

Anti-CD3-AlexaFluor®700 (UCHT1), anti-CD4-APC-eFluor®480 (RPAT4), anti-CD69-biotin (FN50), anti-CD127-PerCP-Cy5.5 (eBioRDRS), anti-CD27-APC-eFluor®780 (LG.7F9), anti-CD4-FITC (RPA-T4), anti-CD27-PE-Cy7 (LG.7F9), anti-CD45-APC (2D1), and anti-EpCAM-PE (IB7), anti-FoxP3-PE-Cy7 (PCH101), anti-IL-2-PE-Cy7 (MQ1-17H12), anti-IFNγ-APC-eFluor®780 (4S.B3), anti-TNFα-PerCP-Cy5.5 (Mab11), anti-PD-1-APC (MIH4), anti-PD-L1-PE-Cy7 (MIH1), mIgG1κ-PE-Cy7 (P3.6.2.8.1), anti-CD45RAFITC (HI100), anti-CD45RO-biotin (UCHL1), CD62L-PE-Cy7 (DREG-56), CCR7-APC-efl780 (3D12), anti-CD3 (OKT3), and anti-CD28 (CD28.2) were purchased from eBioscience (San Diego, CA). Anti-CD8-BV510 (RPA-T8) was purchased from BioLegend (San Diego, CA). Anti-CTLA-4-Biotin and anti-Ki67-PerCP-Cy5.5 (B56) were purchased from BD Biosciences (San Diego, CA). Anti-TIM-3-PE (344823) was purchased from R&D systems. Anti-LAG-3-FITC (17B4) was purchased from Enzo Life Sciences International, Inc. (Plymouth Meeting, PA). Anti-CD107a-PE-Cy7 (H4A3) and anti-perforin-PerCP-Cy5.5 (δG9) were purchased from BD Biosciences. Anti-galectin-9 (ab69630) was purchased from Abcam. Control rabbit IgG (BA-1000) was purchased from Vector Labs (Burlingame, CA). Goat-anti-Rabbit IgG-HRP was purchased from Dako (Carpinteria, CA). All antibodies were used per the manufacturer's recommendations.

Ex vivo Phenotyping by Flow Cytometry

Non-adherent cells were stained with Fixable Viability Dye-efluor450 (1:1000 in DPBS; eBioScience) for 30 minutes at 4°C. Cells were incubated 10 minutes in FcRγ Block (eBioScience). For analysis of T-cell exhaustion, cells were split and stained with the following antibody combinations: (1) anti-CD3-Alexafluor700, anti-CD4-Fitc, anti-CD8, anti-PD-1, anti-TIM-3, anti-CD127, anti-CD27-APC-efluor780, and anti-CD69-biotin or (2) anti-CD3-Alexafluor700, anti-CD4-APC-efluor780, anti-CD8, anti-PD-1, anti-TIM-3, and anti-LAG-3 for 25 minutes at 4°C. Anti-CD69-biotin was detected with Streptavidin-PE-TR (15 minutes at 4°C; eBioscience). Cells were resuspended in 1X Fixation/ with 1X Permeabilization Buffer (eBioscience) and stained with either (1) anti-FoxP3 or (2) anti-CTLA-4-biotin and anti-Ki67 (25 minutes at 4°C). Anti-CTLA-4-biotin was detected with

Streptavidin-PE-TR (15 minutes at 4°C). For memory-cell marker analysis, cells were stained for CD3, CD8, PD-1, TIM-3, CD45RA, CD45RO, CD62L, CCR7, and intracellular perforin as described above. For PD-L1 expression analysis, adherent mDTC cells were stained with anti-EpCAM and anti-CD45 and either left unstained or stained with mIgG or anti-PDL-1 (25 minutes at 4°C). BCPAP, an adherent DTC cell line, was used as a positive control for both EpCAM and PD-L1. Stained cells were fixed in 2.5% paraformaldehyde (PFA) (in PBS). Data were acquired using the Gallios 561 flow cytometer (Beckman Coulter, Fullerton, CA). 10-color compensation was achieved using mIgGκ Compbeads (BD Bioscience). Data analysis was performed with FlowJo™ software (Tree Star, Inc., Ashland, OR). Histogram overlays are displayed in unit area to compare populations containing a wide-range of events.

Stimulated Cytokine Production

Non-adherent cells were resuspended in media plus Golgi Plug™ (1:1000; BD Biosciences) and plated at 2.0 $\times 10^5$ cells per well in a 96-well round-bottom plate. Cells were left unstimulated, stimulated with PMA (50 ng/mL; Sigma) plus ionomycin (0.5 μg/mL; Sigma), or stimulated with plate-bound anti-CD3 (5 μg/ml) plus soluble anti-CD28 (2 μg/mL) and incubated for 6 hours (37°C/5.0% CO_2). Cells were harvested, incubated with Fixable Viability Dye, pretreated with FcRγ Block, and stained for CD3, CD4, CD8, PD-1, and TIM-3. Following fixation and permeabilization, cells were stained for intracellular IL2, IFNγ, and TNFα (25 minutes at 4°C). Samples were fixed with 2.5% PFA and analyzed by flow cytometry.

Stimulated Proliferation Studies

Non-adherent cells were resuspended at 5×10^6 cells/ml and loaded with 10 nM 5-(and 6)-Carboxyfluorescein diacetate succinimidyl ester (CFSE; eBioscience) and were plated in media at 2.0×10^5 cells/well in a 96-well round-bottom plate. Samples were stimulated with immobilized anti-CD3 (0.2 or 5 μg/ml) alone or in combination with soluble anti-CD28 (2 μg/ml) or with anti-CD3/anti-CD28 Dynabeads CTS (Life Technologies) at a 1:1 bead to cell ratio. Recombinant human IL2 was added to each well at 30 U/mL (eBioscience), and cells were incubated for 72 hours. Staining was performed for surface CD3, CD4, and CD8. Cells were fixed in 2.5% PFA and analyzed by flow cytometry.

Cytotoxic Potential Studies

Non-adherent cells were plated in media plus Golgi Plug™ (1:1000) at 2.0×10^5 cells/well in a 96-well round-bottom plate and left unstimulated or stimulated with PMA (50 ng/mL) plus ionomycin (0.5 μg/mL) for 4 hours. Anti-CD107a was added at the start of the incubation to detect CD107a within the extracellular membrane throughout the stimulation. Cells were harvested, incubated with Fixable Viability Dye, pretreated with FcRγ Block, and stained for CD3, CD4, CD8, PD-1, and TIM-3. Following fixation and permeabilization, cells were stain for intracellular perforin and IFNγ (25 minutes at 4°C), fixed with 2.5% PFA, and analyzed by flow cytometry.

Galectin-9 Expression Analysis by Immunohistochemistry

TILN specimens were chosen from each patient's archived tissues based on the presence of both overt metastases and tumor-associated lymphocytes. 4 μm tissue sections were deparaffinized and rehydrated. Antigen-retrieval was performed in citrate buffer (10 mM tri-sodium citrate (Sigma), 0.05% Tween-20 (Sigma), pH 6; 15 minutes, 110°C) in a Decloaking Chamber™ (Biocare Medical, Concord, CA). Tissues were incubated with H_2O_2 (3%; 30 minutes) followed by serum block (5% goat serum plus 1% BSA in DPBS; 1 hour) and stained with control rabbit IgG or anti-galectin-9 (4 μg/mL) overnight at 4°C. Anti-Galectin-9 was detected with goat anti-rabbit-HRP and ImmPact™ Diaminobenzidine (DAB; Vector Labs). Tissues were counterstained with Mayer's hematoxylin (Sigma-Aldrich; St. Louis, MO) and mounted with Cytoseal-XYL (Thermo Scientific). Staining intensity was scored on a 1^+ to 3^+ scale, and the percentage of positive cells was recorded. Allred scores were generated for comparison between samples (24).

Statistical Analysis

To determine the statistical significance of interval data, we used the Mann Whitney nonparametric, two-tailed *t* test. The level of statistical significance, with 95% confidence, was calculated and noted where $p \leq 0.05$ (*) or $p \leq 0.01$. To ensure statistical significance in our flow cytometry analyses (based on Poisson statistics) a minimum of 100 events were collected in the populations of interest.

Results

mDTC-associated PD-1$^+$ CD8$^+$ and CD4$^+$ T cells display a molecular profile indicative of exhaustion

Clinical details of the 12 patients with mDTC are summarized in Table 1. As shown in Figure 1A, $CD8^+$ or $CD4^+$ $CD3^+$ T cells isolated from TILNs were assessed for expression of PD-1. PD-1^+ T-cell levels were absent or low in frequency in PB ($CD8^+$: 0.8 ± 0.8; $CD4^+$: 0.6 ± 0.6), normal lymph nodes (nLN) ($CD8^+$: 0.2 ± 0.2; $CD4^+$: 1.7 ± 0.4), and Patients 4, 6, 7, and 8 ($CD8^+$: 2.9 ± 2.0; $CD4^+$: 3.6 ± 2.1). In the remaining patients, PD-1^+ T-cell frequencies were elevated and ranged from 5% to 38% and from 4% to 33% of the $CD8^+$ (18.0 ± 14.0; p = 0.03) and $CD4^+$ (16.1 ± 11.0; p = 0.02) subsets, respectively. PD-1^+ and PD-1^- T cells were compared for expression of Tim-3, CD69, CD127, and CD27 (Figure 1A and B). Where PD-1^+ cells were too low in frequency to be characterized, the expression of these molecules was assessed in total $CD8^+$ or $CD4^+$ subsets. Tim-3 was not expressed by T cells in the PD-1^{lo} group but was co-expressed at uniformly high levels by PD-$1^+$$CD8^+$ T cells in patients 1, 2, 3, and 11 and at varied levels in Patients 5, 9, 10, and 12. In Patients 2 and 3, PD-$1^-$$CD8^+$ T cells also expressed Tim-3. As expected, T cells in the PD-1^{lo}/Tim-3^- group contained a mixed profile of activated ($CD69^{hi}$, $CD27^{lo}$) and naïve or resting ($CD69^{lo}$, $CD27^{hi}$) cells. This profile was similar to that in normal LNs, although $CD69^{hi}$ T cells were more frequent in TILNs. In contrast, $CD8^+$ T cells from the PD-1^+Tim-3^+ group showed signs of exhaustion. Specifically, CD69 was expressed at uniformly high levels by PD-1^+ T cells. A significant portion of PD-1^- $CD4^+$ and $CD8^+$ T cells from patients 2 and 3 up-regulated CD69, suggesting that these LNs were highly reactive despite the presence of advanced metastases. CD27 remained highly expressed by

both PD-1^{-} and PD-1^{+} CD8^{+} T cells from the PD-1^{+}/Tim-3^{+} group. A statistically significant reduction in CD127 expression was evident in PD-1^{+} CD8^{+} T cells from PD-1^{+}/Tim-3^{+} TILNs compared to that in normal LNs (Figure 1B). Intracellular CTLA-4 was expressed at low levels by PD-1^{+}CD8^{+} T cells from patients 1, 2, 3, 5, 11, and 12. CTLA-4 expression was also observed on a subset of PD-1^{-}CD8^{+} T cells from patients 2 and 3 and by a subset of CD8^{+} T cells from patient 7. Analysis of the CD4^{+} T-cell population revealed CD69, CD127, and CD27 expression profiles that were similar to patient-matched CD8^{+} T cells. However, Tim-3 and PD-1 were clearly co-expressed only in patients 2, 3, 11, and 12. CTLA-4 expression was more robust in the CD4^{+} T-cell subset of both groups, likely due to the inclusion of CD4^{+} Tregs in this analysis. PD-1^{+}CD4^{+} T cells were uniformly CTLA-4^{+} in patients 1, 2, 3, 5, 11 and 12 and also evident in a subset of CD4^{+} T cell in patients 4, 7, and 8. Collectively, these data suggest that PD-1 expression is a sign of T-cell exhaustion in mDTC.

To further characterize mDTC-associated T cells, we assessed CD45RA, CD45RO, CCR7, and CD62L expression (Supplementary Figure 1). CD4^{+} and CD8^{+} T cells from TILNs contained both naïve CD45RA^{+} and memory CD45RO^{+} subsets, similar to that in normal LNs. CCR7^{hi} memory cells were evident in Patient 11, and CD62L^{+} memory cells were found at a high frequency, more comparable to that observed in blood, in both TILNs. PD-1^{+}CD8^{+} T cells from patients 11 and 12 were largely CD45RA^{-}RO^{+} memory cells. The majority of these cells lacked CCR7^{-} and expressed variable levels of CD62L. Thus, PD-1^{+} T cells from TILNs were primarily effector-memory T cells (T_{EM} ; CD45RO^{+}/CCR7^{-}/CD62L$^{+/-}$) that had encountered antigens and differentiated within the TILNs or had migrated following activation (25).

CD8^{+} T cells from PD-1^{+} Tim-3^{+} samples are variably deficient in their ability to produce IL2, TNFα, and IFNγ

To determine whether the presence of PD-1^{+} T cells was associated with compromised cytokine production, we compared production of IL2, TNFα, and IFNγ by T cells from the PD-1^{lo}Tim-3^{-} and PD-1^{+}Tim-3^{+} TILN groups described above. PD-1 and Tim-3 were up-regulated following stimulation *in vitro* (Supplementary Figure 2), compromising our ability to specifically analyze the inherent PD-1^{+}Tim-3^{+} populations (Figure 1). Despite short-term activation in culture, CD8^{+} T cells from PD-1^{+}Tim-3^{+} TILNs were generally compromised in their ability to produce IL2 and TNFα compared to that in PD-1^{lo}Tim-3^{-} TILNs following PMA/ionomycin stimulation (Figure 2A-2C). This trend was evident when gating on total CD8^{+} T cells and PD-1^{+} subsets, and most obvious when comparing PD-1^{+}Tim-3^{+} subsets. The frequencies of IL2^{+} and TNFα^{+} CD8^{+} T cells were variable among PD-1^{+}Tim-3^{+} TILNs. In contrast to the other PD-1^{+}Tim-3^{+} TILNs, CD8^{+} T cells from patient 5 contained a frequency of IL2^{+} and TNFα^{+} similar to that observed in PD-1^{lo}Tim-3^{-} TILNs when stimulated with PMA/Ionomycin (Figure 2C) or anti-CD3/anti-CD28 (Figure 2D). IFNγ^{+} T cells frequencies were not significantly reduced in PD-1^{+}Tim-3^{+} TILNs following PMA/ionomycin stimulation (Figure 2E); however, the IFNγ response was significantly lower when cells were stimulated with anti-CD3/anti-CD28 (Figure 2F). In line with our findings for IL2 and TNFα, IFNγ production was maintained in Patient 5 (Figure 2F, arrows). Cytokine production by CD4^{+} T cells was comparable in

PD-1^{lo}Tim-3^{-} and PD-1^{+}Tim-3^{+} TILNs following PMA/ionomycin stimulation (Figure 2G). Although a subset of PD-1^{+}Tim-3^{+} samples showed markedly reduced IL2 production following anti-CD3/anti-CD28 stimulation, a statistically significant difference was not observed (Figure 2H). Of note, cytokine production by patient PB T cells was variable but comparable between the PD-1^{lo}Tim-3^{-} and PD-1^{+}Tim-3^{+} groups (Supplementary Figure 3). Cytokine levels were significantly lower in normal lymph nodes (Supplementary Figure 3), likely due to the high percentage of naïve T cells. Our comparison of PD-1^{lo}Tim-3^{-} and PD-1^{+}Tim-3^{+} TILNs suggests that expression of molecular markers of exhaustion was associated with impaired cytokine production by CD8^{+} T cells. However, the degree of dysfunction was variable and did not occur in all patients or in tumor-associated PD-1^{+}CD4^{+} T cells.

Proliferative potential is maintained in mDTC-associated CD8^{+} and CD4^{+} T cells

To determine whether mDTC-associated T cells were compromised in their proliferative capacity, we assessed Ki67 by flow cytometry. In agreement with our previous studies in archived TILN tissues (4), a small percentage of T cells expressed Ki67. As shown in Figure 3A, the percentages of Ki67^{+} CD8^{+} and CD4^{+} T cells were similar in PD-1^{lo}Tim-3^{-} and PD-1^{+}Tim3^{+} TILNs. In PD-1^{+}Tim3^{+} TILNs, Ki67^{+} cells were predominantly found in the PD-1^{+} population of CD8^{+} T cells (Figure 3B) and CD4^{+} T cells (data not shown). To determine their proliferative potential *ex vivo*, we stimulated CFSE-labeled non-adherent cells from TILNs for 3 days in the presence anti-CD3/anti-CD28-coated beads and IL2. CD8^{+} T cells from patients 3, 5, 10, and 11 displayed a strong proliferative response that was only minimally reduced compared to PB-derived T cells (Figure 3C). A similar trend was observed in the CD4^{+} T cells from these patients. T cells from patient 9 showed an enhanced response compared to patient blood-derived T cells. The proliferative potential of T cells from patient 8, the only PD-1^{lo}Tim-3^{-} sample available for analysis, was comparable to that of control blood-derived T cells. Results were similar at lower bead:cell ratios (1:5 or 1:10) or in the absence of IL2 (data not shown). To interpret our results in the context of previous T-cell exhaustion studies in human cancers, we also assessed proliferation of mDTC-associated T cells from patient 11 in response to plate-bound anti-CD3 at low and high concentrations and anti-CD3 in combination with soluble anti-CD28 (Figure 3C). Low concentration anti-CD3 was a weak stimulant, driving only one division in normal PB T cells after 3 days. Only 26% of CD4^{+} T cells from patient 11 had divided. Of note, CD8^{+} T cells were significantly reduced in number in both blood and TILN samples when stimulated with 0.2 μg/ml anti-CD3 (data not shown). Under stronger stimulatory conditions (5 μg/ml anti-CD3 and anti-CD3/anti-CD28), the proliferative response was slightly delayed in both CD8^{+} and CD4^{+} T cells from TILNs compared to that from control blood. Despite this delay, more than 96% of CD8^{+} T cells and 60% of CD4^{+} T cells had undergone at least one division by day 3. Thus, while mDTC-associated T cells were less responsive to sub-optimal stimulation, proliferative capacity was largely preserved in response to moderate and strong stimuli *ex vivo*.

Cytotoxic potential may be compromised in CD8^{+} T cells from PD-1^{+} Tim-3^{+} samples

We next assessed the ability of mDTC-associated PD-1^{+}Tim-3^{+} CD8^{+} T cells to degranulate. *Ex vivo* cytotoxic potential is commonly measured by CD107a mobilization to

the cell surface (26). As shown in Figure 4A, 9.5% of PB $CD8^+$ T cells had undergone degranulation following stimulation with PMA/ionomycin. In line with this finding, 9.1% of PB $CD8^+$ T cells expressed intracellular perforin at baseline, and perforin expression was reduced to less than 1% following stimulation and exocytosis (Figure 4B). 16-49% of $CD8^+$ T cells from PD-1^+Tim-3^+ samples (patients 10, 11, and 12) mobilized CD107a to the cell surface (Figure 4A). Of note, CD107a mobilization was most evident in the PD-1^+ and PD-1^+Tim-3^+ $CD8^+$ T-cell subsets in both PB and TILNs (Figure 4A, column 3). Surprisingly, mDTC-associated $CD8^+$ T cells showed no evidence of intracellular perforin (Figure 4B). As expected, perforin expression in PB $CD8^+$ T cells was confined to $CD45RA^+CCR7^-$ T_{EMRA} and, to a lesser extent, $CD45RO^+CCR7^-$ T_{EM} subsets (Figure 4C) (25). Perforin expression was absent in T_{EMRA} (data not shown) and T_{EM} (Figure 4) in TILNs, regardless of PD-1 expression. These data suggest that although PD-1^+Tim-3^+ $CD8^+$ T cells are capable of degranulation, their cytotoxic potential may be diminished.

PD-L1 and galectin-9 are expressed by metastatic DTC

PD-1 and Tim-3 inhibit T-cell function upon ligation of their requisite ligands, PD-L1 and galectin-9 (27-29). As shown in Figure 5, we assessed PD-L1 expression by adherent cell populations derived from TILNs using flow cytometry. Tumor cells were identified by expression of epithelial-cell adhesion molecule (EpCAM) (Figure 5A). BCPAP, a DTC cell line, displayed uniformly low expression of EpCAM but high expression of PD-L1. Primary tumor cells were readily distinguished by their high EpCAM expression, and 9 of 10 tumors expressed PD-L1 to varying degrees (Figure 5A and 5B). No correlation was observed between PD-L1 expression levels and the frequency of PD-1^+CD4^+ or PD-1^+CD8^+ T cells (data not shown). While adherent cells from 2 PD-1^+Tim-3^+ TILNs displayed relatively high levels of PD-L1, expression was not statistically different between PD-1^{lo}Tim-3^- and PD-1^+Tim-3^+ groups (Figure 5B, $p = 0.2571$). A subset of $CD45^+$ tumor-associated leukocytes that remained in the adherent cell cultures displayed low levels of PD-L1, in 4 of 10 samples analyzed (Figure 5A and 5C). In contrast, $CD45^+$ leukocytes from normal lymph nodes lacked PD-L1 expression (Figure 5A). As shown in Figure 5D, galectin-9 was evident on both mDTC and tumor-associated leukocytes. Galectin-9 expression was similar between PD-1^{lo}Tim-3^- and PD-1^+Tim-3^+ TILNs in both mDTC (6.1 ± 0.3 vs. 6.3 ± 0.5, $p = 0.8101$) and leukocytes (5.9 ± 0.6 vs. 4.9 ± 1.1, $p = 0.1227$; Supplementary Table 1). Leukocytes in normal lymph nodes stained at a similar intensity (Figure 5D and Supplementary table 1). Thus, both PD-L1 and galectin-9 are commonly expressed in TILNs and may contribute to immune dysfuction.

Tregs are present at similar frequencies in both PD-1^{lo} Tim-3^- and PD-1^+ Tim-3^+ TILNs

Our previous studies using fine-needle aspirate biopsies (FNAB) revealed that $FoxP3^+CD25^+CD127^{lo}$CTLA-4^+ Tregs were elevated on average in TILNs ($15.4 \pm 6.3\%$) compared to UILNs ($10.3\% \pm 3.6\%$) (4). To investigate the role of Tregs in this study, we assessed FoxP3 expression and other key phenotypic markers of Tregs by flow cytometry. As shown in Figure 6, $FoxP3^+$ Tregs were prominent in all TILN samples, ranging from 12.6-39.0% of the $CD4^+$ T cells ($29.5 \pm 3.8\%$). These levels were significantly higher than that seen in patient-matched PB (Figure 6B; $3.1 \pm 0.5\%$) and normal LNs (Figure 6B; $5.0 \pm 1.6\%$) and were elevated compared to our previous analysis of UILNs and TILNs. Tregs

were present at similar frequencies in both PD-1^{lo}Tim-3^{-} and PD-1^{+}Tim-3^{+} TILNs (Figure 6B; 29.5 ± 3.8% vs. 23.2 ± 3.5%; p = 0.26). CD127 expression was comparable in Tregs from blood, normal LNs, and TILNs. Tregs expressed low levels of PD-1 in samples 2, 3, 7, 8, 9, and 10 and high levels of Tim-3 in 6 of 12 patients. Tim-3 was also expressed by a subset of Tregs in normal LNs. Expression of PD-1 and Tim-3 has been associated with activated and highly suppressive Tregs (30, 31). These data suggest that Tregs may play a key role in the establishment of T-cell exhaustion (32) in PD-1^{+}Tim-3^{+} TILNs and may create an additional barrier to tumor elimination by the immune system in mDTC.

Discussion

Although PD-1^{+} T cells have been found in association with many cancers, functional T-cell exhaustion has been characterized in only a subset of these studies (8-17). Here, we report variable defects in cytokine production by PD-1^{+}CD8^{+} T cells isolated from TILNs in patients with mDTC. Although T cells from Patient 5 displayed a molecular profile of exhaustion, their ability to produce cytokines was unimpaired. Of note, the PD-1^{+}CD8^{+} T cells in this sample contained a definitive PD-1^{+}Tim-3^{-} population. While these data suggest that expression of multiple inhibitory receptors is necessary for reduced T-cell function, co-expression of PD-1 and Tim-3 by CD4^{+} T cells (patients 2 and 3) did not confer a dysfunctional phenotype. Our data lend further support to the theory that expression of molecular markers of exhaustion (PD-1, Tim-3, CD69^{hi}, CD27^{hi}) does not translate uniformly to impaired function (13, 33).

Viral and tumor models suggest that reduced cytotoxic potential occurs during the process of T-cell exhaustion. Specifically, reduced perforin expression was characteristic of exhausted CD8^{+} T cell in chronic LCMV infection (7). Furthermore, perforin was absent in melanoma-specific CD8^{+} T cells from 6 of 9 TILNs (16). It is tempting to conclude that the lack of perforin expression in mDTC-associated CD8^{+} T cells is another sign of functional exhaustion. However, our analysis found no evidence of perforin expression in normal LNs (data not shown) or in the PD-1^{-} T_{EM} population. Further analyses using reactive normal LN tissue and PD-1^{lo}Tim-3^{-} TILNs are required to determine whether the absence of perforin expression is due to tumor-induced T-cell exhaustion or inherent properties of LN tissue.

Studies in other types of cancer have shown that expression of PD-1 and Tim-3 by tumor-associated T cells results in reduced proliferative capacity (10, 13, 17). In follicular B-cell non-Hodgkin's lymphoma, only 10% of Tim-3^{+}CD8^{+} and 8% of Tim-3^{+}CD4^{+} T cells had undergone at least one division after 72 hours compared to 45% of Tim-3^{-}CD8^{+} and 23% of Tim-3^{-}CD4^{+} T cells following stimulation with immobilized anti-CD3 (0.2 μg/ml). CLL-associated CD8^{+} T cells were defective in proliferation following stimulation with anti-CD3 (5 μg/ml) and anti-CD28 (13). In 7 of 20 CLL samples tested, the percentage of CD8^{+} T cells that had undergone division was less than 25%. CD8^{+} T-cell proliferation in the remaining 13 samples was similar to that observed in normal healthy controls. In our analyses using multiple stimulation regimens, we observed a subtle delay in T-cell proliferation in a subset of patients. However, more than 86% had undergone at least one division following anti-CD3/anti-CD28 stimulation. This is in sharp contrast to the markedly

reduced $CD8^+$ T-cell proliferative responses observed in CLL. These data suggest that proliferative capacity is largely maintained in mDTC-associated T cells, despite enrichment of PD-1^+Tim-3^+ cells. Taken together, our functional analyses lead us to conclude that $CD8^+$ T-cell exhaustion is incomplete in patients with mDTC and may be readily reversible.

T cells from PD-1^{lo}Tim-3^- TILNs showed no evidence of phenotypic exhaustion or functional defect *ex vivo*. Surprisingly, the size and frequency of metastatic tumors were similar in PD-1^{lo}Tim-3^- and PD-1^+Tim-3^+ TILNs (Table 1). This paradox may be explained by the following hypotheses: 1) It is possible that, despite activation by professional antigen-presenting cells, tumors have escaped detection in these patients. High expression of CD69 by a significant portion of T cells in 3 of the 4 PD-1^{lo}Tim-3^- TILNs suggests that these cells have undergone activation. Given the extent of tumor load in these LNs, it is probable that these activated T cells are reactive to the tumor rather than to unrelated pathogens. However, the tumor cells may have down-regulated their own antigen processing and presentation machinery necessary for immune recognition. 2) T cells may be compromised (i.e., anergy and/or senescence) *in vivo* but not *ex vivo*. Functional defects may be reversed once the T cells are removed from the tumor microenvironment and exposed to non-physiologic stimuli. In support of this hypothesis, Tregs, PD-L1, and galectin-9 were also evident in PD-1^{lo}Tim-3^- TILNs and likely encourage immune dysfunction. 3) It is conceivable that T-cell exhaustion is a common theme in all TILNs but that signs of exhaustion are not evident in all samples at the time of analysis. Specifically, our characterization of PD-1^{lo}Tim-3^- TILNs may have taken place at the early stages of exhaustion where function is largely maintained and inhibitory receptors are not yet up-regulated. It is likely that *ex vivo* restimulation with physiologically relevant antigen would reveal an even broader continuum of dysfunction among mDTC patients. Additional studies are required to characterize alternative mechanisms of T-cell dysfunction and tumor escape in mDTC.

As described above, regional mDTC appears to be slow-growing and poorly metastatic, but persists without elimination by the host immune system. Our studies suggest that, in the majority of patients with grossly-involved LNs, tumor-reactive T cells are actively engaging the tumor. Although ineffective in elimination, this response likely impedes tumor growth and metastases. The degree of functional exhaustion was variable in patients with evident PD-1^+Tim-3^+ T-cell enrichment and may be reversible in the majority of cases. We suggest that immune-modulating therapies that inhibit PD-1/PD-L1 and/or Tim-3/galectin-9 are viable options for patients with persistent disease. These checkpoint therapies may also inhibit the suppressive activity of Tregs (34, 35). Current PD-1/PD-L1-targeted therapies display low toxicities, and if injected locally into TILNs via ultrasound guidance, may be even more tolerable (36-38).

While these studies focus on regional mDTC, we expect that PD-1/PD-L1-targeted therapies may be effective in patients with aggressive localized DTC and distant metastatic disease that cannot be cured by standard therapies (i.e., surgery, radioactive iodine, or tyrosine kinase inhibitors (TKI)). The vascular-endothelial growth factor receptor 2 (VEGFR2) inhibitor sorafenib, was successful in slowing tumor growth, but did not achieve durable responses (39). Future studies are necessary to characterize the immune response in

aggressive DTC and to investigate the potential for PD-1/PD-L1 blockade and TKI combination therapy.

Supplementary Material

Refer to Web version on PubMed Central for supplementary material.

Acknowledgments

Financial Support:

Severson, JJ: N/A

Serracino, HS: N/A

Mateescu, V: N/A

Raeburn, CD: N/A

McIntyre, RC: N/A

Sams, SB: N/A

Haugen, BR: Mary Rossick Kern and Jerome H. Kern Endowment in Endocrine Neoplasms Research

French, JD: American Thyroid Association THANC grant 2009 American Cancer Society IRG #57-001-50NIH/NCRR Colorado CTSI Grant #UL1 RR025780

References

1. Howlader, N.; NA; Krapcho, M.; Neyman, N.; Aminou, R.; Waldron, W.; Altekruse, SF., et al., editors. Surveillance Epidemiology and End Results (SEER): Cancer Statistics Review 1975-2008. National Cancer Institute; Bethesda, MD: 2011. http://seer.cancer.gov/csr/1975_2008, based on November 2010 SEER data submission, posted to the SEER web site
2. Mazzaferri EL, Jhiang SM. Long-term impact of initial surgical and medical therapy on papillary and follicular thyroid cancer. Am J Med. 1994; 97:418–28. [PubMed: 7977430]
3. Ito Y, Jikuzono T, Higashiyama T, Asahi S, Tomoda C, Takamura Y, et al. Clinical significance of lymph node metastasis of thyroid papillary carcinoma located in one lobe. World J Surg. 2006; 30:1821–8. [PubMed: 16983469]
4. French JD, Kotnis GR, Said S, Raeburn CD, McIntyre RC Jr. Klopper JP, et al. Programmed Death-1+ T Cells and Regulatory T Cells Are Enriched in Tumor-Involved Lymph Nodes and Associated with Aggressive Features in Papillary Thyroid Cancer. J Clin Endocrinol Metab. 2012; 97:E934–43. [PubMed: 22466343]
5. Wherry EJ. T cell exhaustion. Nat Immunol. 2011; 12:492–9. [PubMed: 21739672]
6. Wherry EJ, Blattman JN, Murali-Krishna K, van der Most R, Ahmed R. Viral persistence alters CD8 T-cell immunodominance and tissue distribution and results in distinct stages of functional impairment. J Virol. 2003; 77:4911–27. [PubMed: 12663797]
7. Wherry EJ, Ha SJ, Kaech SM, Haining WN, Sarkar S, Kalia V, et al. Molecular signature of CD8+ T cell exhaustion during chronic viral infection. Immunity. 2007; 27:670–84. [PubMed: 17950003]
8. Ahmadzadeh M, Johnson LA, Heemskerk B, Wunderlich JR, Dudley ME, White DE, et al. Tumor antigen-specific CD8 T cells infiltrating the tumor express high levels of PD-1 and are functionally impaired. Blood. 2009; 114:1537–44. [PubMed: 19423728]
9. Baitsch L, Baumgaertner P, Devevre E, Raghav SK, Legat A, Barba L, et al. Exhaustion of tumor-specific CD8(+) T cells in metastases from melanoma patients. J Clin Invest. 2011; 121:2350–60. [PubMed: 21555851]

10. Fourcade J, Sun Z, Benallaoua M, Guillaume P, Luescher IF, Sander C, et al. Upregulation of Tim-3 and PD-1 expression is associated with tumor antigen-specific CD8+ T cell dysfunction in melanoma patients. J Exp Med. 2010; 207:2175–86. [PubMed: 20819923]
11. Fourcade J, Sun Z, Pagliano O, Guillaume P, Luescher IF, Sander C, et al. CD8+ T Cells Specific for Tumor Antigens Can Be Rendered Dysfunctional by the Tumor Microenvironment through Upregulation of the Inhibitory Receptors BTLA and PD-1. Cancer Res. 2012; 72:887–96. [PubMed: 22205715]
12. Matsuzaki J, Gnjatic S, Mhawech-Fauceglia P, Beck A, Miller A, Tsuji T, et al. Tumor-infiltrating NY-ESO-1-specific CD8+ T cells are negatively regulated by LAG-3 and PD-1 in human ovarian cancer. Proc Natl Acad Sci U S A. 2010; 107:7875–80. [PubMed: 20385810]
13. Riches JC, Davies JK, McClanahan F, Fatah R, Iqbal S, Agrawal S, et al. T cells from CLL patients exhibit features of T-cell exhaustion but retain capacity for cytokine production. Blood. 2013; 121:1612–21. [PubMed: 23247726]
14. Wang SF, Fouquet S, Chapon M, Salmon H, Regnier F, Labroquere K, et al. Early T Cell Signalling Is Reversibly Altered in PD-1 T Lymphocytes Infiltrating Human Tumors. PLoS One. 2011; 6:e17621. [PubMed: 21408177]
15. Zhang Y, Huang S, Gong D, Qin Y, Shen Q. Programmed death-1 upregulation is correlated with dysfunction of tumor-infiltrating CD8+ T lymphocytes in human non-small cell lung cancer. Cell Mol Immunol. 2010; 7:389–95. [PubMed: 20514052]
16. Zippelius A, Batard P, Rubio-Godoy V, Bioley G, Lienard D, Lejeune F, et al. Effector function of human tumor-specific CD8 T cells in melanoma lesions: a state of local functional tolerance. Cancer Res. 2004; 64:2865–73. [PubMed: 15087405]
17. Yang ZZ, Grote DM, Ziesmer SC, Niki T, Hirashima M, Novak AJ, et al. IL-12 upregulates TIM-3 expression and induces T cell exhaustion in patients with follicular B cell non-Hodgkin lymphoma. J Clin Invest. 2012; 122:1271–82. [PubMed: 22426209]
18. Blackburn SD, Shin H, Haining WN, Zou T, Workman CJ, Polley A, et al. Coregulation of CD8+ T cell exhaustion by multiple inhibitory receptors during chronic viral infection. Nat Immunol. 2009; 10:29–37. [PubMed: 19043418]
19. Brooks DG, Teyton L, Oldstone MB, McGavern DB. Intrinsic functional dysregulation of CD4 T cells occurs rapidly following persistent viral infection. J Virol. 2005; 79:10514–27. [PubMed: 16051844]
20. Crawford A, Angelosanto JM, Kao C, Doering TA, Odorizzi PM, Barnett BE, et al. Molecular and Transcriptional Basis of CD4(+) T Cell Dysfunction during Chronic Infection. Immunity. 2014; 40:289–302. [PubMed: 24530057]
21. Kassu A, Marcus RA, D'Souza MB, Kelly-McKnight EA, Golden-Mason L, Akkina R, et al. Regulation of virus-specific CD4+ T cell function by multiple costimulatory receptors during chronic HIV infection. J Immunol. 2010; 185:3007–18. [PubMed: 20656923]
22. Kaufmann DE, Kavanagh DG, Pereyra F, Zaunders JJ, Mackey EW, Miura T, et al. Upregulation of CTLA-4 by HIV-specific CD4+ T cells correlates with disease progression and defines a reversible immune dysfunction. Nat Immunol. 2007; 8:1246–54. [PubMed: 17906628]
23. Goding SR, Wilson KA, Xie Y, Harris KM, Baxi A, Akpinarli A, et al. Restoring immune function of tumor-specific CD4+ T cells during recurrence of melanoma. J Immunol. 2013; 190:4899–909. [PubMed: 23536636]
24. Phillips T, Murray G, Wakamiya K, Askaa J, Huang D, Welcher R, et al. Development of standard estrogen and progesterone receptor immunohistochemical assays for selection of patients for antihormonal therapy. Appl Immunohistochem Mol Morphol. 2007; 15:325–31. [PubMed: 17721279]
25. Sallusto F, Lenig D, Forster R, Lipp M, Lanzavecchia A. Two subsets of memory T lymphocytes with distinct homing potentials and effector functions. Nature. 1999; 401:708–12. [PubMed: 10537110]
26. Betts MR, Brenchley JM, Price DA, De Rosa SC, Douek DC, Roederer M, et al. Sensitive and viable identification of antigen-specific CD8+ T cells by a flow cytometric assay for degranulation. J Immunol Methods. 2003; 281:65–78. [PubMed: 14580882]

27. Dong H, Strome SE, Salomao DR, Tamura H, Hirano F, Flies DB, et al. Tumor-associated B7-H1 promotes T-cell apoptosis: a potential mechanism of immune evasion. Nat Med. 2002; 8:793–800. [PubMed: 12091876]

28. Keir ME, Liang SC, Guleria I, Latchman YE, Qipo A, Albacker LA, et al. Tissue expression of PD-L1 mediates peripheral T cell tolerance. J Exp Med. 2006; 203:883–95. [PubMed: 16606670]

29. Zhu C, Anderson AC, Schubart A, Xiong H, Imitola J, Khoury SJ, et al. The Tim-3 ligand galectin-9 negatively regulates T helper type 1 immunity. Nat Immunol. 2005; 6:1245–52. [PubMed: 16286920]

30. Gupta S, Thornley TB, Gao W, Larocca R, Turka LA, Kuchroo VK, et al. Allograft rejection is restrained by short-lived TIM-3+PD-1+Foxp3+ Tregs. J Clin Invest. 2012; 122:2395–404. [PubMed: 22684103]

31. Raimondi G, Shufesky WJ, Tokita D, Morelli AE, Thomson AW. Regulated compartmentalization of programmed cell death-1 discriminates CD4+CD25+ resting regulatory T cells from activated T cells. J Immunol. 2006; 176:2808–16. [PubMed: 16493037]

32. Jin HT, Jeong YH, Park HJ, Ha SJ. Mechanism of T cell exhaustion in a chronic environment. BMB Rep. 2011; 44:217–31. [PubMed: 21524346]

33. Badoual C, Hans S, Merillon N, Van Ryswick C, Ravel P, Benhamouda N, et al. PD-1-expressing tumor-infiltrating T cells are a favorable prognostic biomarker in HPV-associated head and neck cancer. Cancer Res. 2013; 73:128–38. [PubMed: 23135914]

34. Amarnath S, Mangus CW, Wang JC, Wei F, He A, Kapoor V, et al. The PDL1-PD1 axis converts human TH1 cells into regulatory T cells. Sci Transl Med. 2011; 3:111ra120.

35. Kitazawa Y, Fujino M, Wang Q, Kimura H, Azuma M, Kubo M, et al. Involvement of the programmed death-1/programmed death-1 ligand pathway in CD4+CD25+ regulatory T-cell activity to suppress alloimmune responses. Transplantation. 2007; 83:774–82. [PubMed: 17414712]

36. Brahmer JR, Drake CG, Wollner I, Powderly JD, Picus J, Sharfman WH, et al. Phase I study of single-agent anti-programmed death-1 (MDX-1106) in refractory solid tumors: safety, clinical activity, pharmacodynamics, and immunologic correlates. J Clin Oncol. 2010; 28:3167–75. [PubMed: 20516446]

37. Fransen MF, Sluijter M, Morreau H, Arens R, Melief CJ. Local activation of CD8 T cells and systemic tumor eradication without toxicity via slow release and local delivery of agonistic CD40 antibody. Clin Cancer Res. 2011; 17:2270–80. [PubMed: 21389097]

38. Hamid O, Robert C, Daud A, Hodi FS, Hwu WJ, Kefford R, et al. Safety and tumor responses with lambrolizumab (anti-PD-1) in melanoma. N Engl J Med. 2013; 369:134–44. [PubMed: 23724846]

39. Brose MS, Nutting CM, Jarzab B, Elisei R, Siena S, Bastholt L, et al. Sorafenib in radioactive iodine-refractory, locally advanced or metastatic differentiated thyroid cancer: a randomised, double-blind, phase 3 trial. Lancet. 2014; 384:319–28. [PubMed: 24768112]

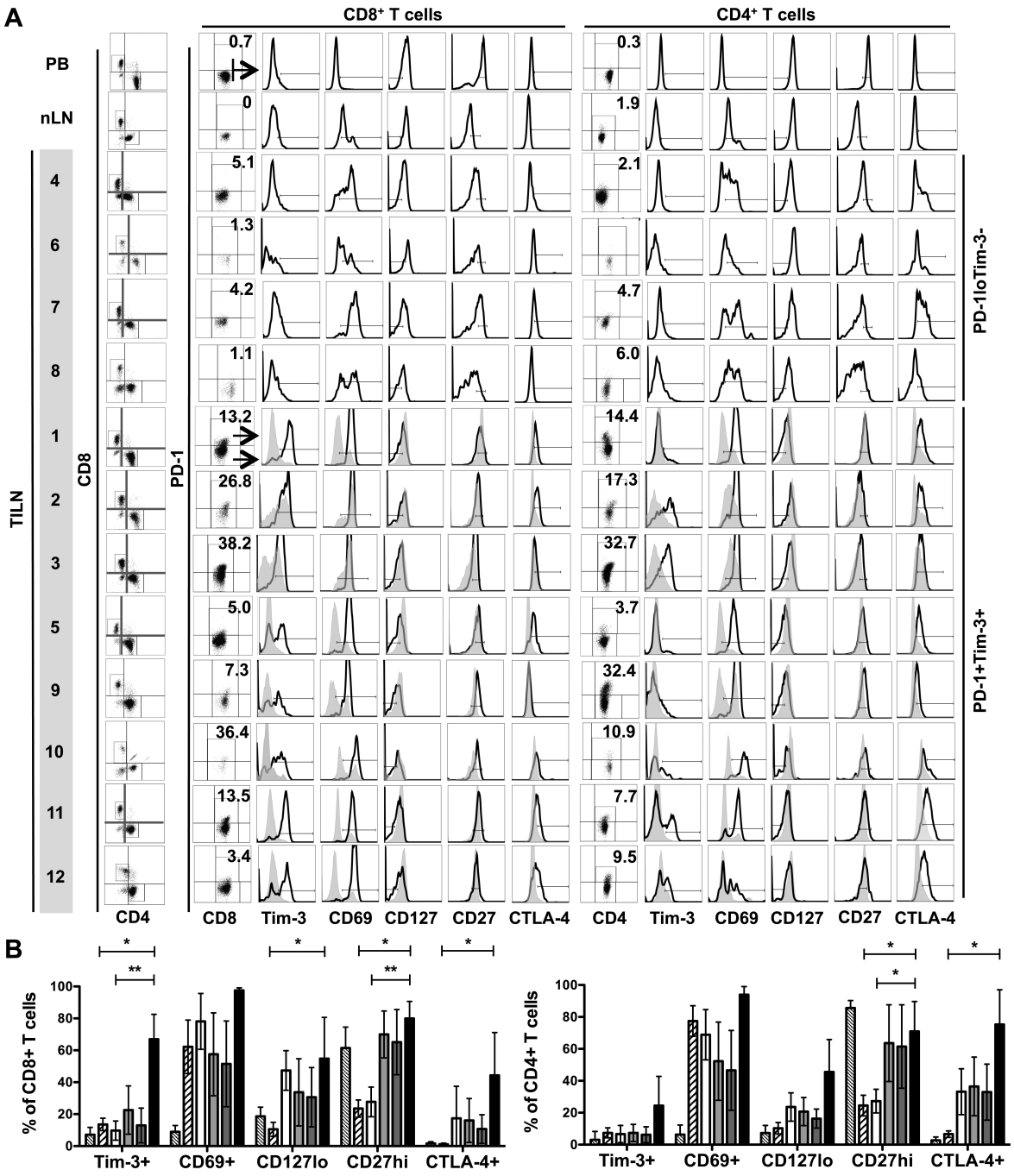

Figure 1. Phenotype of T Cells Isolated from TILNs

T cells from PB, normal lymph node (nLN), and TILN sections from 12 mDTC patients were analyzed by flow cytometry. (A) Viable $CD8^+$ T cells and $FoxP3^-CD4^+$ T cells were analyzed for PD-1 expression (%$PD\text{-}1^+$ is noted). Total $CD8^+$ or $FoxP3^-CD4^+$ populations were analyzed for the designated receptors in Patients 4, 6, 7, and 8 whose $PD\text{-}1^+$ cells were too infrequent to assess ($PD\text{-}1^{lo}Tim\text{-}3^-$). In the remaining samples ($PD\text{-}1^+Tim\text{-}3^+$), $PD\text{-}1^+$ (black line) and $PD\text{-}1^-$ (filled grey histogram) subpopulations were compared. $FoxP3^+$ Tregs were included in the analysis of intracellular CTLA-4 expression. PB samples were used to

determine the gating strategy. (B) Combined analysis of PB (thin hatched), nLN (thick hatched), PD-1^{lo}Tim-3^{-} TILN (white), and PD-1^{+}Tim-3^{+} TILN (light grey) or PD-1^{-} (dark gray) and PD-1^{+} (black) subsets in PD-1^{+}Tim-3^{+} TILN. * $p \leq 0.05$; ** $p \leq 0.01$

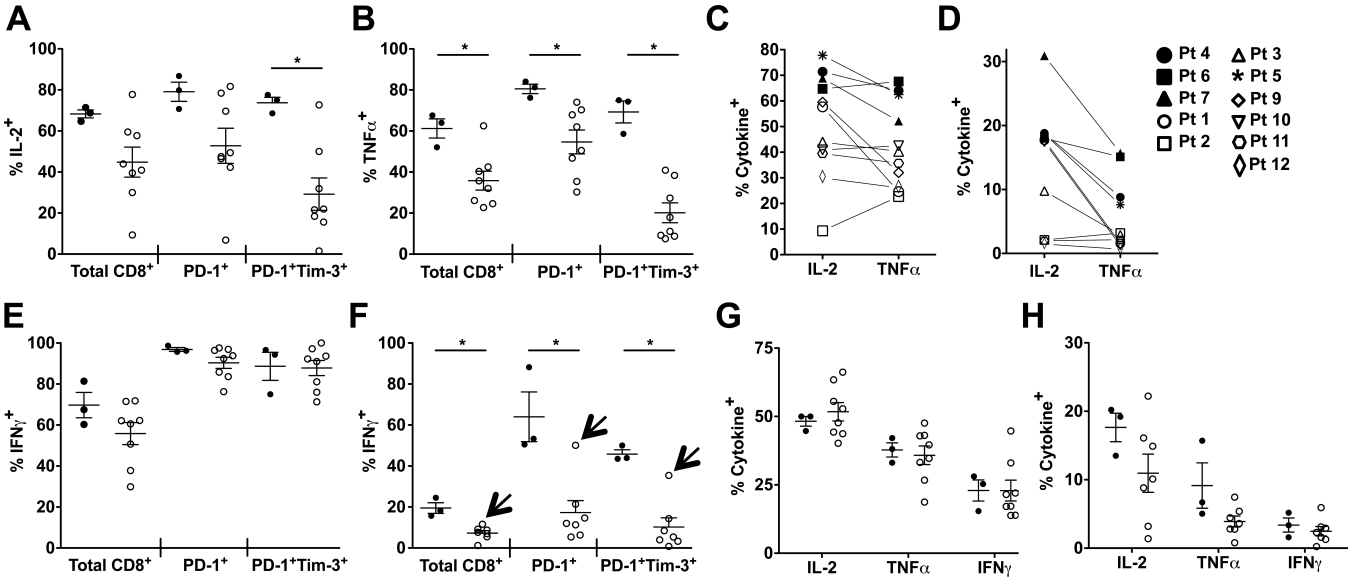

Figure 2. Stimulated Cytokine Production in T Cells Isolated from TILNs

Total $CD8^+$ T cell and $PD\text{-}1^+$ or $PD\text{-}1^+Tim\text{-}3^+$ subsets from $PD\text{-}1^{lo}Tim\text{-}3^-$ (filled circles) and $PD\text{-}1^+Tim\text{-}3^+$ (open circles) TILNs were compared following stimulation with PMA/ionomycin for frequencies of $IL2^+$ (A) or $TNF\alpha^+$ (B) cells. Percentages of total $CD8^+$ T cells expressing IL2 or TNFα are shown for each patient following PMA/ionomycin (C) or anti-CD3/anti-CD28 (D) stimulation. The percentage of $IFN\gamma^+$ cells are shown for total $CD8^+$ T cells and $PD\text{-}1^+$ or $PD\text{-}1^+Tim\text{-}3^+$ subsets following PMA/ionomycin (E) or anti-CD3/anti-CD28 (F) stimulation. Arrows designate the values for Patient 5. The percentage of $cytokine^+$ cells are shown for total $CD4^+$ T cells following PMA/ionomycin (G) or anti-CD3/anti-CD28 (H) stimulation. Mean and SEM are shown. * $p \leq 0.05$

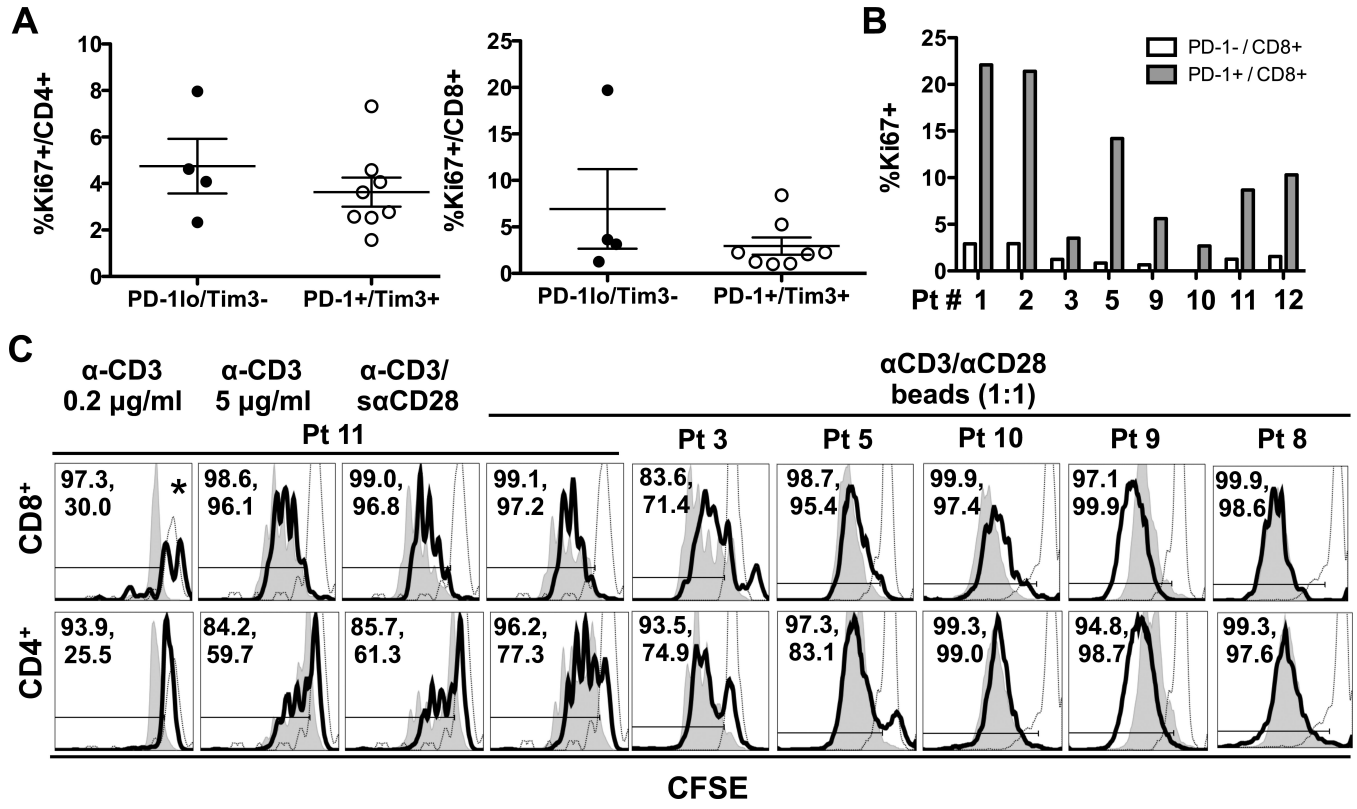

Figure 3. Proliferation profiles of T cells recovered from TILNs

Non-adherent cells from TILNs were analyzed by flow cytometry for expression of Ki67. (A) Percent Ki67$^+$ of total CD8$^+$ or total CD4$^+$ T cells is compared between PD-1^{lo}Tim-3$^-$ and PD-1$^+$Tim-3$^+$ TILN groups. Mean and SEM are shown. (B) Percent Ki67$^+$ in PD-1$^-$ and PD-1$^+$ CD8$^+$ T-cell subsets is shown for all PD-1$^+$Tim-3$^+$ patient (Pt) samples. (C) Non-adherent cells from TILN samples (black line) were compared to those in patient or normal PB (filled grey histogram) in an *ex vivo* proliferation assay. CD3$^-$ cells in the PB population were used to define the undivided CFSE^{hi} population (open grey histograms). The percentage of cells that had undergone at least one division is noted (PBMCs, TILNs). *Fewer than 100 events were collected in the CD8$^+$ T-cell gate from TILNs.

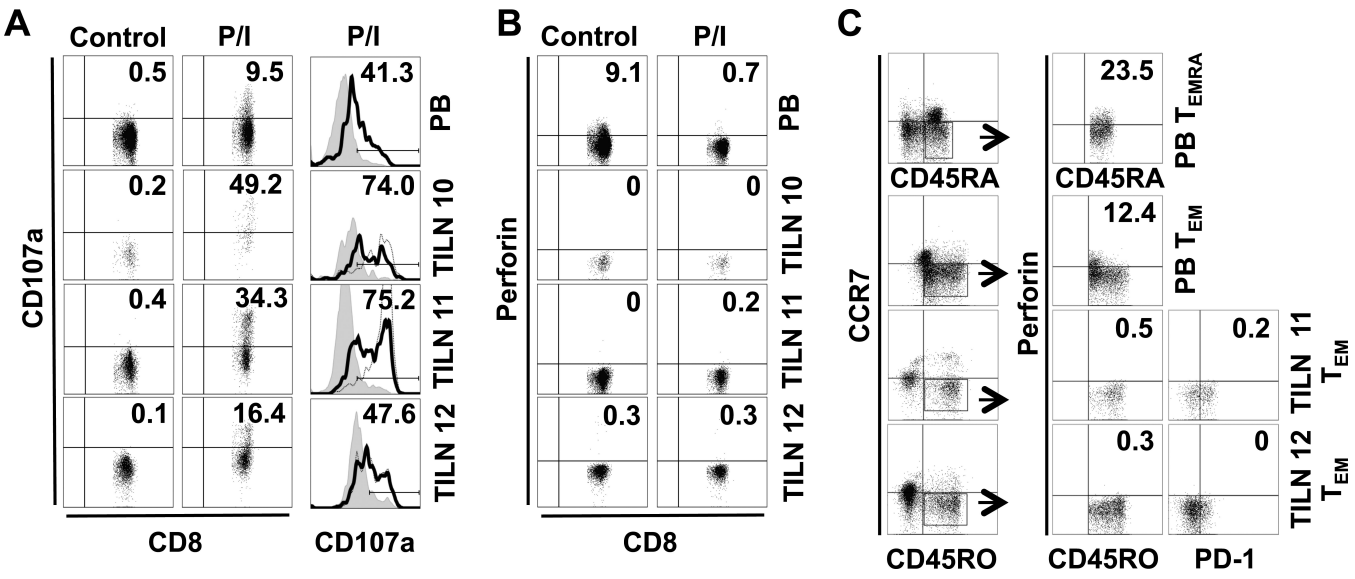

Figure 4. Cytotoxic potential of CD8$^+$ T cells from PD-1$^+$Tim-3$^+$ TILNs

T cells from normal PB or TILNs were left unstimulated (control) or stimulated with PMA and ionomycin (P/I). (A) Viable CD8$^+$ T cells were for CD107a expression by flow cytometry (percent positive is noted). CD107a expression levels in PD-1$^-$ (filled grey histogram), PD-1$^+$(black line; percent positive is shown), and PD-1$^+$Tim-3$^+$ (dotted line) subsets were compared following stimulation. (B) Corresponding intracellular perforin levels are shown. (C) Unstimulated CD8$^+$ T cells were analyzed for expression of memory markers. TEMRA and TEM populations were further analyzed for intracellular perforin and PD-1 expression.

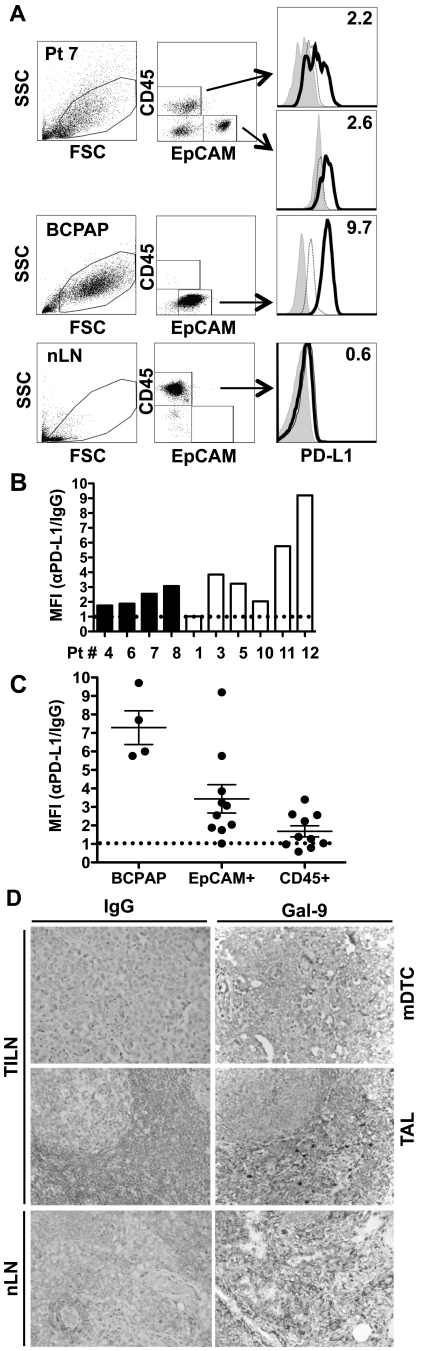

Figure 5. PD-L1 and galectin-9 expression in TILNs

(A) Viable EpCAM^{+} tumor cells and CD45^{+} leukocytes that remained in the adherent cells from TILNs were gated and analyzed for PD-L1 expression by flow cytometry. Patient (Pt) 7 is shown as a representative sample. PD-L1 (black line) is compared to IgG (dotted line) or unstained (grey histogram) controls. Fold median fluorescence index (MFI) of anti-PD-L1/IgG is noted. (B) Relative PD-L1 expression is shown for each PD-1^{lo}Tim-3^{-} (black bars) or PD-1^{+}Tim-3^{+} (white bars) TILN. (C) Combined analysis of 4 experiments is shown. The dotted line denotes the threshold for PD-L1 expression. (D) Representative images of

galectin-9 expression in TILNs (Patient 1; 40X magnification) and normal LN (nLN). mDTC = metastasis; TAL = mDTC-associated leukocytes.

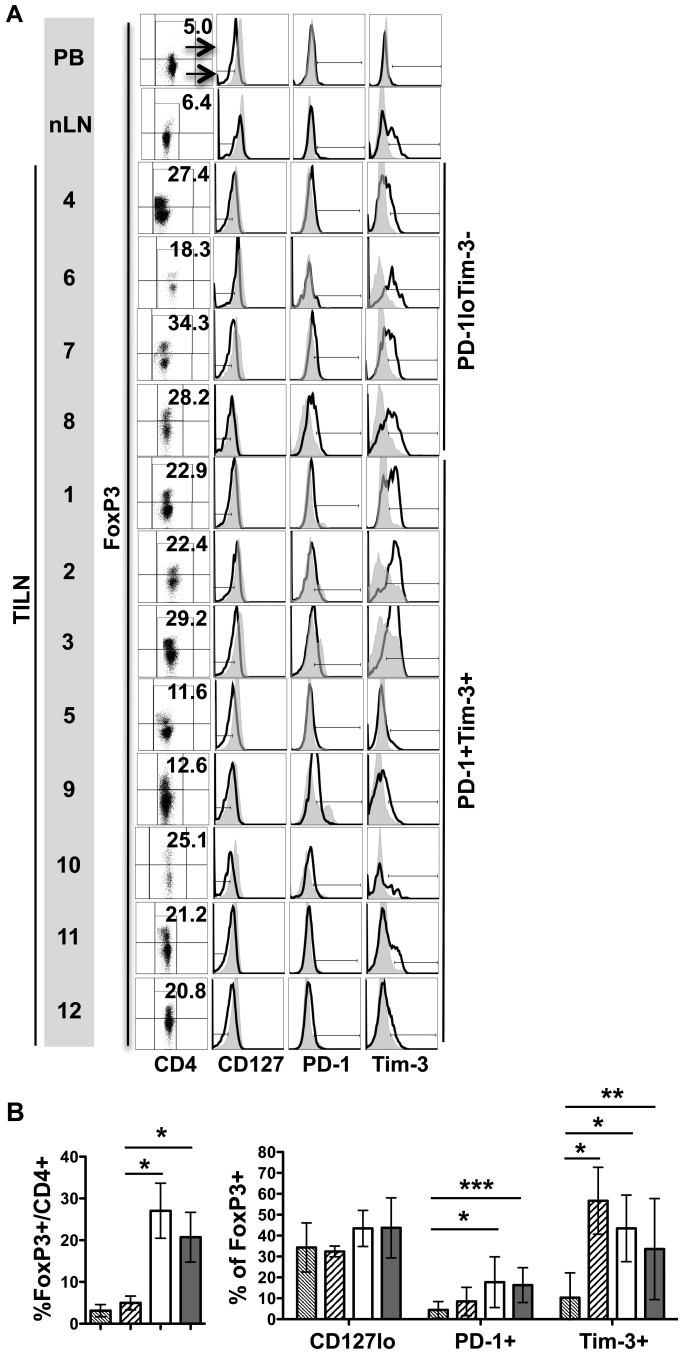

Figure 6. Treg frequency and phenotype in TILNs

(A) The percentage of FoxP3^{+} cells in the total CD4^{+} T-cell population was determined by flow cytometry. FoxP3^{+} Tregs (black line) and FoxP3^{-} (filled grey histogram) subsets were compared for expression of CD127, PD-1, and Tim-3. (B) Combined analysis of Treg frequency and activation markers in PB (thin hatched), normal lymph node (thick hatched), PD-1^{lo}Tim-3^{-} TILNs (white), and PD-1^{+}Tim-3^{+} TILNs (light grey).

Table 1

Clinical Summary and $CD8^+$ T Cell Phenotype.

Patient	LN Source	Age	Gender	TNM Staging	Primary (P) or Recurrent (R)	TILN/Total LN (%)	Extranodal Extension	Largest Met (cm)	Phenotype
1	CND	33	F	pT3 pN1bM0	P	36/83 (43)	Y	2	PD-1+/Tim-3+
2	RLND	25	F	pT3 pN1bM0	P	14/58 (24)	Y	2.2	PD-1+/Tim-3+
3	CND, RLND	31	F	pT4a pN1b MX	P	4/65* (6)	Y	2.1	PD-1+/Tim-3+
4	CND, RLND	59	M	pT3 pN1bM0	P	34/65 (57)	Y	2.2	PD-1lo/Tim-3-
5	CND	48	F	pT1 pN1aM0	R (7 months)	7/7 (P); 36/86 (R) (45)	N	1.3	PD-1+/Tim-3+
6	CND	37	F	pT3 pN1bM0	R (7 months)	2/12 (P); 7/10 (R) (41)	Y	1.1	PD-1lo/Tim-3-
7	CND, LLND	24	F	pT3 pNlbMX	P	28/73 (38)	Y	2.5	PD-1lo/Tim-3-
8	CND	79	M	pTXpN1bM1	R (10 months)	2/26 (P); 2/9 (R)* (11)	Y	2.1	PD-1lo/Tim-3-
9	CND, LLND	48	F	pT3 pNlbMX	P	8/72(11)	N	0.4	PD-1+/Tim-3+
10	LLND	53	M	pT3 pNlbMX	P	3/45 (7)	ND	0.4	PD-1+/Tim-3+
11	CND, LLND	27	M	pT3 pN1bM0	P	77/141 (55)	Y	2.5	PD-1+/Tim-3+
12	CND, LLND	29	F	pT1 pN1a MX	P	28/108 (26)	N	0.4	PD-1+/Tim-3+

CND (Central Neck Dissection); RLND (Right Lateral Neck Dissection); LLND (Left Lateral Neck Dissection). For recurrent patients, the time from initial treatment to surgery for recurrence is noted in parentheses.

* denotes samples where LNs were matted due to tumor metastasis and determination of LN number was compromised. Patients categorized as $PD\text{-}1^+Tim\text{-}3^+$ are highlighted in grey.